Effect of annealing temperature on the performance of ZnO thin film-based dye sensitized solar cell

Cite as: AIP Conference Proceedings **2267**, 020010 (2020); https://doi.org/10.1063/5.0015699
Published Online: 21 September 2020

May Zin Toe, Atsunori Matsuda, Soe Soe Han, Khatijah Aisha Yaacob, and Swee-Yong Pung

Effect Of Annealing Temperature On The Performance Of ZnO Thin Film-Based Dye Sensitized Solar Cell

May Zin Toe[1], Atsunori Matsuda[2], Soe Soe Han[3], Khatijah Aisha Yaacob[1], Swee-Yong Pung[1, a)]

[1]*School of Materials and Mineral Resources Engineering, Engineering Campus, Universiti Sains Malaysia, 14300 Nibong Tebal, Penang, Malaysia*
[2] *Department of Electrical and Electronic Information Engineering, Toyohashi University of Technology, 1-1 Hibarigaoka, Tempaku-cho, Toyohashi 441-8580, Japan*
[3]*University of Yangon, Kamayut, 11041, Yangon, Yangon Region, Myanmar*

[a)]Corresponding Author: sypung@usm.my

Abstract.TiO_2 based dye sensitized solar cells suffer from fast electrons recombination rate. ZnO, which has wide bandgap energy that similar to TiO_2 (E_g = 3.3 eV) and a higher mobility of electron may overcome the issue suffered by TiO_2. In this work, ZnO thin film-based dye sensitized solar cells were fabricated. The ZnO thin films were dip-coated on the FTO substrate followed by annealing. The effect of annealing temperature on the morphology, optical and their DSSC's performance were studied. The result showed that DSSC made of ZnO thin film annealed at 450°C recorded the best power conversion efficiency of 0.68%.

1. INTRODUCTION

Dye-sensitized solar cells (DSSCs) are currently one of the most efficient third-generation solar technology available[1]. Third-generation solar technologies include organic photovoltaics (OPVs) [2], copper zinc tin sulphide (CZTS) [3], perovskite solar cells [4], DSSCs [5] and quantum dot solar cells [6]. A DSSC is a low-cost solar cell, consisting of semiconductor based photoanode, photosensitized dye and an electrolyte [7]. The most studied semiconductor based photoanode is titanium dioxide (TiO_2) [8], followed by zinc oxide (ZnO) based photoanode [9].

ZnO is II-VI group compound semiconductor. Many ZnO-based applications have been reported such as ZnO based thin film transistor [10], biosensors [11], photocatalyst [12], short wavelength light-emitting devices [13] and dye-sensitized solar cell [14-16]. It is a potential replacement for TiO_2 as both materials have same electron affinities, identical bandgap energies (TiO_2: 3.2 eV and ZnO: 3.3eV), large excitation binding energy (60 meV) and higher electron mobility (115-155 $cm^2V^{-1}s^{-1}$) [17]. Unlike TiO_2, the anisotropic growth of ZnO that produce nanorods and nanowires, making it a prime material for DSSCs due to better electrons transportation.

ZnO thin film is normally deposited on conductive thin oxide (CTO) glass substrates such as fluorine doped tin oxide (FTO) coated glass for the fabrication of photoanode. In addition, the ZnO thin film could be used as seed layer to reduce the lattice mismatch between ZnO and FTO substrate, and facilitate the subsequent growth of ZnO nanorods. Many deposition methods have been used to deposit ZnO thin films. These deposition methods include chemical vapour deposition (CVD) [18], sputtering [19], pulsed laser deposition (PLD) [19], thermal evaporation [20], and sol-gel [21]. Nevertheless, deposition of ZnO thin films using dip-coating method attracts attention of researchers because it is an environmentally friendly process, simple, low cost and potentially for mass production [22, 23].

In this work, zinc acetate were dip-coated on the FTO glass substrates. Subsequently, it was annealed for 60 minutes in normal atmosphere in order to oxidize the zin acetate into ZnO. Various annealing temperatures were used, i.e. 350, 450, 550 and 650 °C. The effect of annealing temperature on the formation of ZnO thin films, their respective morphology, optical property and power conversion efficiency of DSSCs were studied.

3rd International Postgraduate Conference on Materials, Minerals & Polymer (MAMIP) 2019
AIP Conf. Proc. 2267, 020010-1–020010-8; https://doi.org/10.1063/5.0015699
Published by AIP Publishing. 978-0-7354-2030-4/$30.00

2. EXPERIMENTAL METHOD

2.1 Deposition of ZnO Thin Films

FTO substrates were cut into size of 2cm x 3cm. The substrates were ultrasonic cleaned using 2-proponal, ethanol and distilled water. Subsequently, the substrates were pre-heated at 250°C for 10 minutes on the hot plate in order to remove residual of water and solvent on its surface. The zinc acetate solution was prepared by mixing zinc acetate dehydrate, diethanolamine, deionized water and 2-proponal followed the molar ratio of 1:1:1:20. The solution was stirred continuously at room temperature for 1 hour. A clear and homogeneous sol solution was obtained. The sol was coated on the FTO substrate by dip coater (Aiden) with down-speed of 5 mm/s, holding time for 10s and withdrawing speed of 0.1mm/s. After that the sol coated substrates were dried at room temperature and then placed in oven at 100 °C for 15 minutes. The dip coating process was repeated for 3 cycles to achieve homogeneous, uniform and good surface coverage of sol on the surface of FTO substrates. Finally, the sol-coated films were annealed at different annealing temperatures i.e. 350, 450, 550 and 650°C for 60 minutes to form ZnO thin films on the FTO substrates.

The crystal structure of ZnO thin films were characterized by X-ray diffraction (XRD, Rigaku RINT 2500). The morphology and cross-section of the ZnO thin films were examined using Field Emission Scanning Electron Microscope (FE-SEM, HITACHI, S-4800). The thin film sheet resistances were analysed by Resistivity Processor (Model-NPS ∑ -5+). The optical properties of ZnO thin films were analysed using an ultraviolet-visible spectrophotometer (V-670, JASCO Corporation) and Raman spectroscope (NRS-3100, JASCO Corporation).

2.2 Fabrication of ZnO Thin Film Based DSSC

The ZnO thin film coated FTO substrates (photoanodes/working electrode) were immersed in the mixture of 0.3 mM of N719 dye (Sigma Aldrich; 65 mol% dioxole) and ethanol solution for 1 day. After soaking with dye, the working electrodes were rinsed with distilled water for several times and dried at room temperature. The counter electrodes were prepared by sputtering Pt sputtered for 10 minutes on FTO coated substrate. The DSSCs were assembled by placing the two substrates, i.e. the working electrode (ZnO thin film) and the counter electrode (Pt) as illustrated in Fig. 1. The two substrates were sealed with thermal adhesive (50 μm). The electrolyte composed of 0.05 M iodine (WAKO), 0.1 M lithium iodide (WAKO), 0.6 M 1,2-di-methyl-3-propylimidazolium iodide (WAKO) and 0.5 M 4-tert-butylpyridine and acetonitrile (WAKO) (solvent). It was injected into the cell through one of the two small holes drilled on the Pt counter electrode. Subsequently, the holes were sealed using polytetrafluoroethylene sealant to prevent leakage of the electrolyte. The current density-voltage (J-V) curves were measured by ADCMT 6244 DC Voltage/Current Source/Monitor and an HAL–320 W solar simulator (Asahi spectra) with a 300 W xenon lamp and an air-mass 1.5 global filter. The incident light intensity and active area was kept at 100mW/cm^2 and 1(1 x 1) cm^2, respectively.

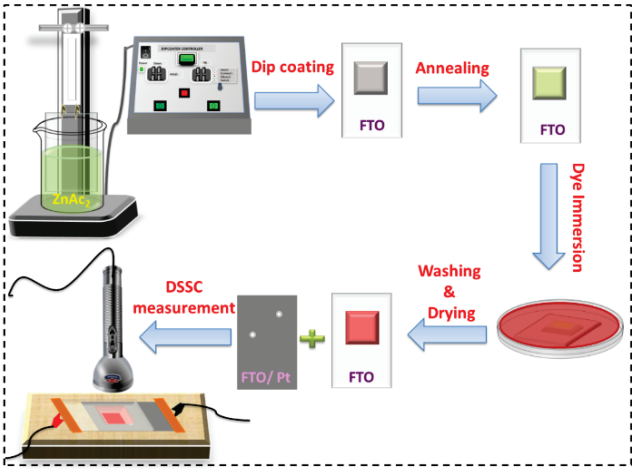

FIGURE 1. Schematic diagram of the fabrication process of ZnO thin film based DSSCs.

3. RESULTS AND DISCUSSION

Figure 2 shows the XRD results of as-deposited thin film and thin films annealed at 350, 450, 550 and 650 °C for 60 minutes. Except diffraction peaks of FTO (JCPDF 98-006-3707), no ZnO diffraction peaks could be observed for as-deposited thin film and thin film annealed at 350 °C. The result suggests that annealing temperature up to 350 °C was insufficient to form ZnO although the decomposition of zinc acetate is 300 °C [24]. Nevertheless, diffraction peaks that matched with ZnO (JCPDF 96-100-0063) were detected for thin films annealed between 450-650 °C. The annealing temperature was sufficient to decompose and oxidize zinc acetate into ZnO as described in Eq. (1).

$$Zn(O_2CCH_3)_2.2H_2(s) + 4O_2(g) \xrightarrow{\Delta} ZnO(s) + 4CO_2(g) + 5H_2O(g) \quad (1)$$

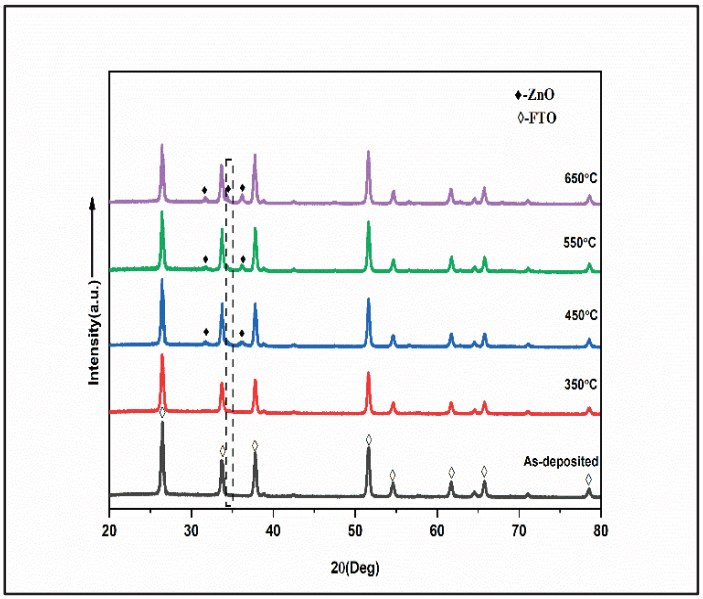

FIGURE 2. XRD patterns ZnO thin films deposited on FTO substrates at various annealing temperatures.

The main diffraction peak of ZnO is (002) as highlighted in dotted square box in Fig. 2. The (002) has the lowest surface free energy, resulting the fastest growth direction that perpendicular to this crystal plane, i.e. in (0001) direction (c-axis) [25]. The estimated crystallite size using Scherrer's equation is 22 nm. Although higher annealing temperature produced better ZnO thin film, the annealing temperature of 550 and 650°C were not suitable to be used. The FTO glass substrates experienced deformation at these high temperature.

Figure 3 shows the top view of thin films annealed various annealing temperature. The thin films composed of many tiny crystal grains. Generally, the size of crystal grains increased with increasing annealed temperature attributed to Ostwald ripening effect. Similar observation was reported by Husna *et al*. [26]. In addition, higher temperature improved the adhesion of thin films on the FTO glass substrate. As highlighted in the cross sectional view of Fig. 4 (a)-(c), delamination of thin films occurred for annealing temperature below 450 °C. In contrary, the thin film adhered well on the FTO glass substrates when it was annealed at 550 °C and 650 °C. Also, it is noted that the thin films were deposited uniformity on the FTO glass substrates with average thickness of 0.71 µm. This indicates that the dip-coating method provided satisfactory control in the thickness of thin film.

Figure 5 shows the EDX analysis on thin films annealed at various temperatures. It could be seen that the O at. % increased with annealing temperature. More oxygen reacted with Zn to form ZnO at higher temperature. This result agrees well with the XRD analysis in Fig. 2 as more ZnO was produced at higher annealing temperatures.

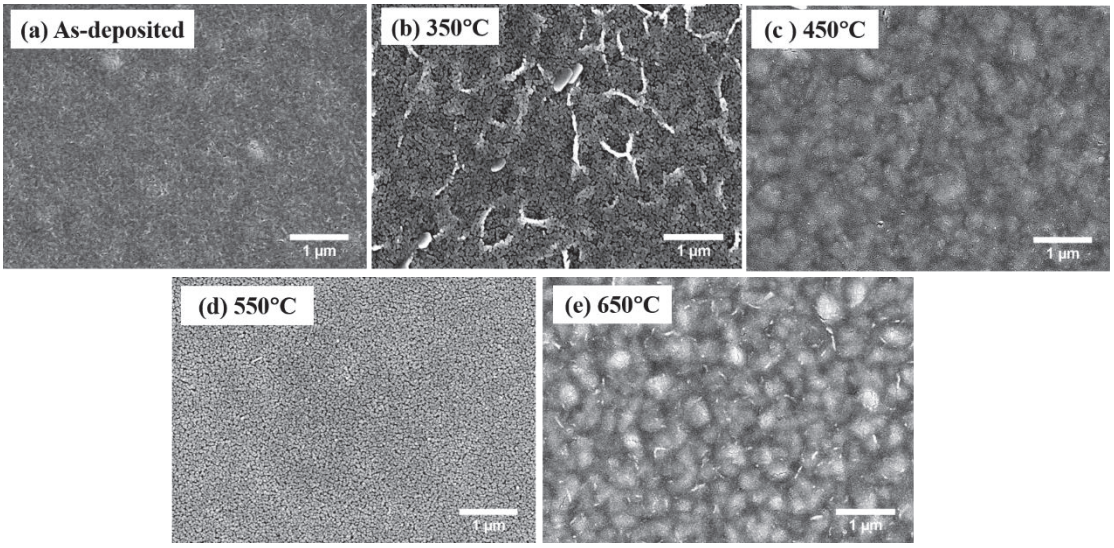

FIGURE 3. Top view of thin films annealed at various annealing temperatures as characterized by FESEM.

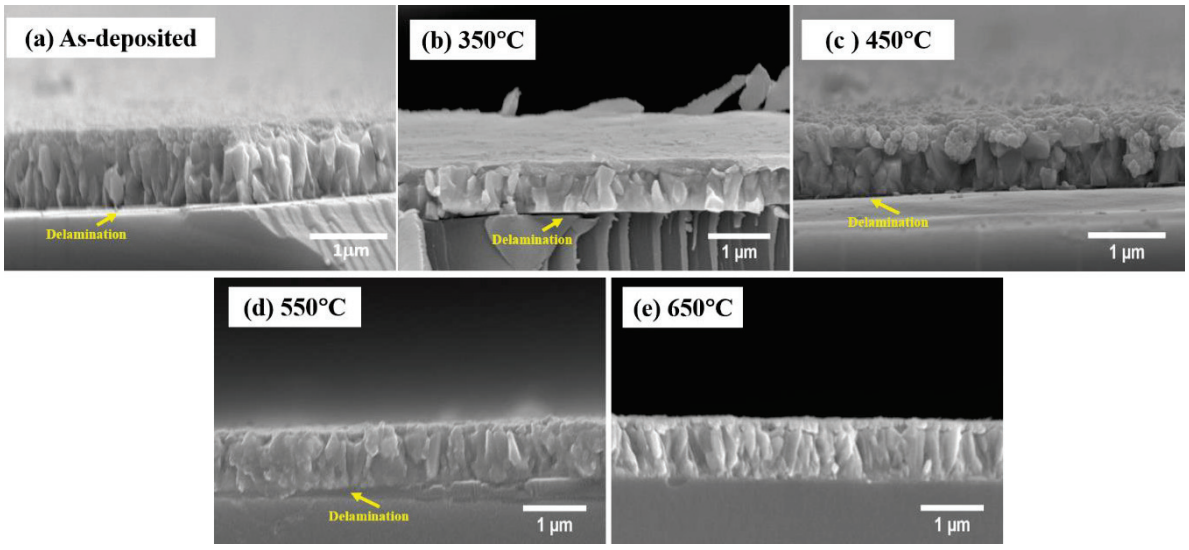

FIGURE 4. Cross-sectional view of thin films annealed at various annealing temperature as characterized by FESEM.

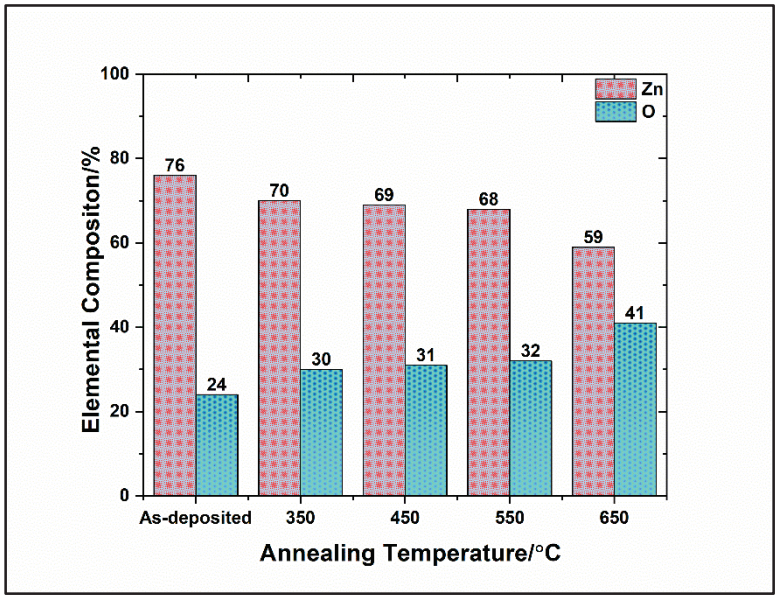

FIGURE 5. EDX analysis of thin films annealed at various annealing temperature.

Raman spectroscopy was used to study the vibrational property of ZnO thin films annealed at various temperatures. As shown in Fig 6, all samples exhibit the same peaks but with slightly different Raman shifts. The peak at approximately 458 cm^{-1} is attributed to the E_2 (high) mode. It was not dominated in the non-resonant Raman scattering spectra, indicating that the ZnO thin films contained a large amount of defects. The peak at 562 cm^{-1} is corresponded to A_1 (LO) mode which could only appear when the c-axis of wurtzite ZnO is parallel to the surface of specimen. The present of 562 cm^{-1} in as-deposited thin film indicates the present of small amount of ZnO, which was not found by XRD attributed to the its detection limit. In general, the increase of intensity for both Raman peaks, i.e. 458 cm^{-1} and 562 cm^{-1} with increasing annealing temperature, suggesting the increase amount of ZnO on the thin film.

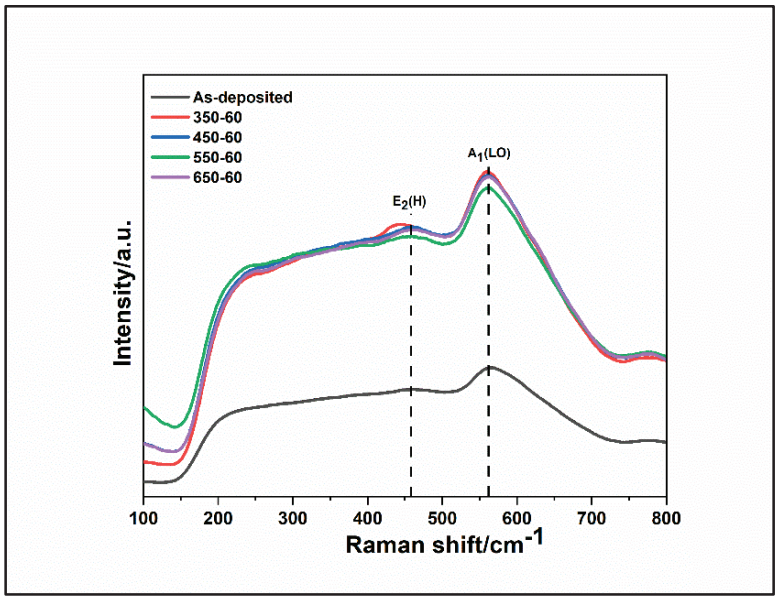

FIGURE 6. Raman spectra of ZnO thin films annealed at various temperature.

Low sheet resistance (high conductivity) thin films are required for the fabrication of DSSCs. Figure 7 shows the influence of annealing temperature on the sheet resistance of ZnO thin films measured by four-probe resistance technique. The sheet resistance was significant decreased from 11.4 Ω/square (as-deposited) to 5.67 Ω/ square (350 °C) with increasing annealing temperature. This was attributed to the formation of ZnO as shown in XRD analysis in Fig. 2. The low sheet resistance of thin film could mainly contribute by high content of zinc interstitials as measured by EDX analysis (Fig. 5). Wei et al. reported similar finding [27]. Nevertheless, the sheet resistance increased again when the annealing temperatures increased up to 650 °C. In brief, although higher annealing temperature improved the quality of ZnO films, it induced higher sheet resistance which did not favor for the fabrication of DSSCs.

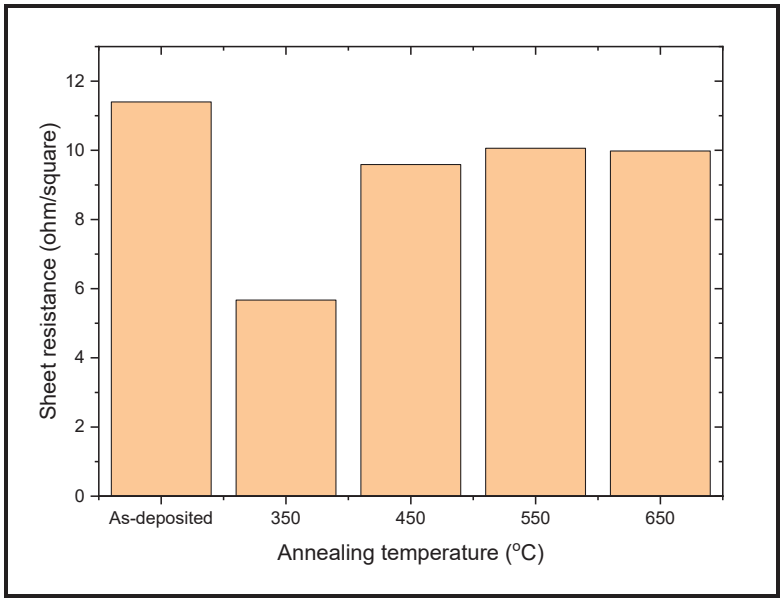

FIGURE 7. Sheet resistance of thin films annealed at various temperature.

Figure 8 shows the current density vs voltage curves of DSSCs fabricated using ZnO thin films that annealed at various temperatures. The power conversion efficiencies (PCE) of each DSSCs were calculated and recorded in Table 1. The result shows that the PCE increased from 0.01 % for as-deposited thin film till the highest PCE of 0.68 % for thin film annealed at 450 °C. The improvement of PCE was attributed to the formation of more ZnO crystals with increasing annealing temperature. The poor performance of DSSCs fabricated using thin films annealed below 450 °C were attributed to the following reasons: (i) present of a large amount of crystal defects from incomplete oxidation of zinc acetate sol and large amount of grain boundaries from tiny crystal grains. These crystal defects acted as recombination centres, reducing the mobility and lifetime of photogenerated electrons, and (ii) delamination of thin films that obstructed the flow of electrons that deteriorated the performance of DSSCs. Nevertheless, the PEC dropped significantly to 0.08 % when thin film was annealed at 550 °C. The deformation of FTO glass substrate at this high temperature, causing warpage of glass substrates was the main cause of this observation. Consequently, it was difficult to maintain the consistency for the gap/space between the working electrode and counter electrode.

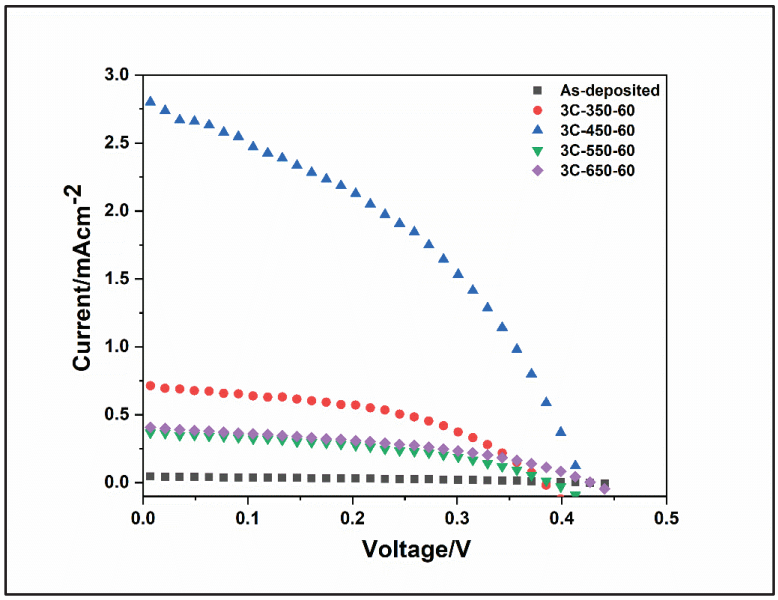

FIGURE 8. Current density - voltage curves of DSSCs fabricated using ZnO thin films annealed at various temperature.

TABLE 1. Performance of ZnO thin film based DSSC

Annealed temperature (°C)	J_{sc} (Ma/cm^2)	V_{oc} (V)	Fill Factor	Conversion efficiency (η%)
As-deposited	0.05	0.42	0.35	0.01
350	0.72	0.49	0.45	0.16
450	2.82	0.59	0.40	0.68
550	0.37	0.50	0.41	0.08
650	0.41	0.55	0.40	0.09

4. CONCLUSION

In this work, the effect of annealing temperature on ZnO thin film based DSSCs are reported. Low annealing temperature (<450 °C) was not suitable as the zinc acetate sol was not decomposed and oxidized completely to form ZnO as indicated in the XRD, EDX and Raman spectroscopy analyses. Also, presence of large amount of crystal

defects in thin films and delamination of thin films at low annealing temperature deteriorated the performance of ZnO thin film based DSSC. DSSC fabricated from ZnO thin film that annealed at 450 ºC achieved the best PEC with efficiency of 0.68 %.

ACKNOWLEDGEMENTS

The authors would like to express appreciation for the financial support from AUN/SEED-Net (Grant number: 304.PBAHAN.6050390/J135), as well as support from the Electrical and Electronic Information Engineering department at the Toyohashi University of Technology(TUT) and School of Materials and Mineral Resources Engineering Campus, Universiti Sains Malaysia.

REFERENCES

1. S. Sharma, K. K. Jain, and A. Sharma, MSA. **6**, 1145 (2015).
2. J. C. Bernede, J. Chil. **53**, 1549-1564 (2008).
3. X. Xin, M. He, W. Han, J. Jung, and Z. Lin, Angew. Chem. Int. Ed. **50**, 11739-11742 (2011).
4. M. Liu, M. B. Johnston, and H. J. Snaith, Nature. **501**, 395 (2013).
5. W. M. Campbell, A. K. Burrell, D. L. Officer, and K. W. Jolley, Coord. Chem. **248**, 1363-1379 (2004).
6. A. Nozik, PHYSICA E. ISSN. **14**, 115-120 (2002).
7. S. Mathew, A. Yella, P. Gao, R. Humphry-Baker, B. F. Curchod, N. Ashari-Astani, I. Tavernelli, U. Rothlisberger, M. K. Nazeeruddin, and M. Grätzel, Nat. Chem. **6**, 242 (2014).
8. A. Wold, Chemistry of Materials. **5**, 280-283 (1993).
9. D. Sengupta, P. Das, K. Usha, B. Mondal, and K. Mukherjee, *Zinc oxide photo-anode based chlorophyll sensitized solar cell*. 2014.
10. E.-J. Yun, H. J. Moon, B. S. Bae, S.-M. Jin, H. G. Nam, and N.-I. Cho, J. Korean Phys. Soc. **60**, 55-58 (2012).
11. S. K. Arya, S. Saha, J. E. Ramirez-Vick, V. Gupta, S. Bhansali, and S. P. Singh, Anal. Chim. Acta. **737**, 1-21 (2012).
12. A. Ramirez-Canon, M. Medina-Llamas, M. Vezzoli, and D. Mattia, PCCP. **20**, 6648-6656 (2018).
13. E. Lai, W. Kim, and P. Yang, Nano Res. **1**, 123-128 (2008).
14. C.-H. Ku and J.-J. Wu, Appl. Phys. Lett. **91**, 093117 (2007).
15. T. Marimuthu, N. Anandhan, R. Thangamuthu, and S. Surya, J. Alloys Compd. **693**, 1011-1019 (2017).
16. C. Velazquez-Gonzalez, E. Armendariz-Mireles, W. Pech-Rodriguez, D. González-Quijano, and E. Rocha-Rangel, Microsyst. Technol. 1-9
17. E. Kaidashev, M. v. Lorenz, H. Von Wenckstern, A. Rahm, H.-C. Semmelhack, K.-H. Han, G. Benndorf, C. Bundesmann, H. Hochmuth, and M. Grundmann, Appl. Phys. Lett. **82**, 3901-3903 (2003).
18. V. Rogé, C. Guignard, G. Lamblin, F. Laporte, I. Fechete, F. Garin, A. Dinia, and D. Lenoble, Catal. Today. **306**, 215-222 (2018).
19. V. Craciun, J. Elders, J. G. Gardeniers, and I. W. Boyd, Appl. Phys. Lett. **65**, 2963-2965 (1994).
20. N. Bouhssira, S. Abed, E. Tomasella, J. Cellier, A. Mosbah, M. Aida, and M. Jacquet, Appl. Surf. Sci. **252**, 5594-5597 (2006).
21. R. R. Søndergaard, M. Hösel, and F. C. Krebs, J POLYM SCI POL PHYS. **51**, 16-34 (2013).
22. G. Valle, P. Hammer, S. H. Pulcinelli, and C. V. Santilli, J. Eur. Ceram. Soc. **24**, 1009-1013 (2004).
23. T. Ratana, P. Amornpitoksuk, and S. Suwanboon, J. Alloys Compd. **470**, 408-412 (2009).
24. A. Zaier, A. Meftah, A. Jaber, A. Abdelaziz, and M. Aida, JKSUS. **27**, 356-360 (2015).
25. S.-Y. Pung, K.-L. Choy, X. Hou, and C. Shan, Nanot. **19**, 435609 (2008).
26. J. Husna, M. M. Aliyu, M. A. Islam, P. Chelvanathan, N. R. Hamzah, M. S. Hossain, M. Karim, and N. Amin, Energy Procedia. **25**, 55-61 (2012).
27. X. Wei, Z. Zhang, M. Liu, C. Chen, G. Sun, C. Xue, H. Zhuang, and B. Man, Mater. Chem. Phys. **101**, 285-290 (2007).